

Interpretation of electronic excitations in coordinated CO systems as observed by electron-energy-loss spectroscopy

H. -J. Freund* and R. P. Messmer

General Electric Corporate Research and Development, Schenectady, New York 12301

W. Spiess, H. Behner, and G. Wedler

*Institut für Physikalische und Theoretische Chemie, Universität Erlangen-Nürnberg,
Egerlandstr.3, 8520 Erlangen, Federal Republic of Germany*

C. M. Kao

Department of Physics, University of Pennsylvania, Philadelphia, Pennsylvania 19104

(Received 18 October 1984; revised manuscript received 26 August 1985)

We present a consistent assignment of the electronic excitations in the electron-energy-loss spectra (EELS) of free and chemisorbed CO. The experimental data (for excitations up to 15 eV) show that for a variety of molecular environments (i.e., free, physisorbed, weakly or strongly chemisorbed) the electronic excitation energies change only slightly. New EELS experimental results for the CO/Fe(110) system are also presented. In order to gain some understanding as to the possible origin of this relative constancy in the excitation energies we have carried out a series of *ab initio* calculations on the ground state and various excited states of CO and NiCO. In the calculations, the generalized valence-bond configuration-interaction method has been employed. On the basis of these calculations it is possible to suggest that when CO is chemisorbed on a metal surface the bond energies of the surface complex for various excited states (arising from $4\sigma \rightarrow 2\pi$ and $5\sigma \rightarrow 2\pi$ excitations) are similar to the bond energy of metal—CO in the ground state. As a consequence, the excitation energies would be expected to be similar for the gas-phase molecule and the chemisorbed molecule, consistent with the experimental findings. Calculations are presented also for a charge-transfer excitation from the metal to the molecule. The concepts used for the valence excitations apply as well for the observed shifts of core-to-bound (C $1s \rightarrow 2\pi$, O $1s \rightarrow 2\pi$) excitations of adsorbed CO, with respect to gas-phase CO. It is suggested that upon chemisorption the relatively large singlet-triplet splitting of the core-to-bound excited states observed in the electron-energy-loss spectra of CO in the gas phase decreases due to interaction with the metal.

I. INTRODUCTION

The assignment of electron-energy-loss spectra¹⁻¹⁵ for the electronic excitations of CO molecularly adsorbed on transition-metal surfaces has recently been a topic of active discussion. A collection of such spectra for a variety of adsorbate systems¹⁻⁷ is shown in Fig. 1. Spectra for both weakly chemisorbed (Cu) (Refs. 3 and 4) and strongly chemisorbed (Ni, Pd, and Fe) (Refs. 3 and 5-7) molecular CO are presented. On the right-hand side of the figure, the energies of the primary electron beams are indicated. The controversy in the literature concerns the assignment of the shaded peaks as opposed to those marked with arrows. Netzer¹⁶ has recently summarized the various assignments, and we shall not repeat all these aspects here. There seems to be a general agreement, however, that the shaded peaks are due to intramolecular excitations on the adsorbed molecule, while those marked with arrows originate mainly (i.e., most of the observed intensity) from charge-transfer excitations between the metal and the molecule. The charge-transfer excitations, of course, have no analog in the free molecule.

The data in Fig. 1 include a high-resolution gas-phase spectrum as well as condensed solid-phase spectra for the

noncoordinated CO molecule. These experimental data show that for a variety of molecular environments (i.e., physisorbed, weakly or strongly chemisorbed), the electronic excitation energies change only slightly with respect to the excitation energies in the gas phase. This suggests that when a CO molecule is bound to a metal surface there is a change in the electronic ground-state energy which is approximately the same as the corresponding changes in the electronic excited-state energies.

The plan of the present paper is given in the following. In Sec. II A we present the experimental methods and new results and in Sec. II B the theoretical methods and new results. In Sec. III A we discuss the gas-phase CO valence spectrum on the basis of existing theoretical calculations.¹⁷⁻²⁰ We then use this information in Sec. III B to obtain an assignment for the intramolecular excitations of CO in the adsorbed cases. For the new case of a strongly chemisorbed system, namely CO on Fe(110) at 77 K,²¹ we are able to identify excitations at $\sim 8-9$ eV and at ~ 13 eV, i.e., at excitation energies again very similar to the CO excitations in the gas phase. Reference is made to the optical-absorption spectra of Ni(CO)₄ (Ref. 22) and Fe(CO)₅ (Ref. 23) to locate and identify charge-transfer excitations in the electron-energy spectra and to discuss

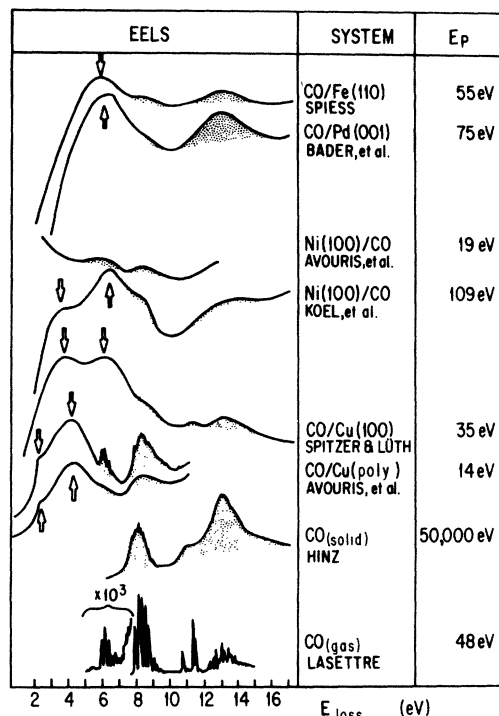


FIG. 1. Collection of EEL spectra of gas phase CO (Ref. 1), solid CO (Ref. 2), CO/Cu(poly) (Ref. 3), CO/Cu(100) (Ref. 14), CO/Ni(100) (Refs. 3 and 5), CO/Pd(100) (Ref. 5), and CO/Fe(110) (Ref. 7). The primary electron energies (E_p) are indicated.

the intensities of the excitations. On the basis of the collected experimental evidence we derive a consistent assignment of CO adsorbate loss spectra, and develop a simple theoretical model to understand the experimental observations. The observed similarities of excitation energies in loss spectra of free and adsorbed CO can be explained by considering the response of the metal electrons to the altered electron distribution in the excited state of the molecule. In order to test the simple theoretical model suggested, results of *ab initio* generalized valence-bond configuration-interaction (GVB-CI) calculations for the ground state and two excited states of free CO are reported and compared with those of the corresponding states of a simple cluster model, namely NiCO.

Some discussion about the motivation for using such a simple cluster model as a basis for studying the electronically excited states of molecules on surfaces is appropriate here. This motivation originates from the success of cluster models as a basis for the interpretation of a variety of spectroscopic properties of molecular adsorbates, such as photoelectron emission and vibrational excitation.^{24,25} Also very recently, Netzer²⁶ presented an electron-energy-loss (EEL) spectrum of condensed $\text{Ir}_4(\text{CO})_{12}$ covering excitation energies up to 20 eV. This spectrum was very similar to the corresponding spectrum of CO/Ir(111),²⁶ indicating that EELS (EEL spectroscopy) mainly probes the local metal-molecule electronic structure. Furthermore, it was recently proposed by Plummer *et al.*²⁷ that the excitation energies measured by EELS correlate with the ionization energies measured by photoelectron spec-

troscopy. Plummer *et al.*²⁷ implied that as far as the CO moiety is concerned, the final screened state in a photoemission experiment on adsorbed CO may be very similar to the state produced by electronic excitation (if the excitation results in the same hole and the same excited orbitals as the ionization-screening process). The difference between the final state in a loss experiment and the screened final state in a photoionized experiment is the presence of a hole on the metal in the case of the photoionized state. It was concluded, therefore, that the electron-loss energies and the ionization energies should differ essentially by the work function of the metal. In other words, the binding energy with respect to the Fermi energy, measured in a photoemission experiment should be identical to the loss energy, except for the spin-decoupling energy of a particular state, by which the ionization energy should be lower.²⁷ The latter is due to the fact that the final doublet state of a photoionization experiment (assuming an initial singlet ground state) allows for both singlet and triplet spin coupling of the hole and the screening electron, which very likely results in the population of the more stable triplet-coupled doublet state. In an electron-energy-loss experiment, however, usually the singlet-coupled excited states have the higher oscillator strengths so that their energies dominate the spectrum.^{3,28,29} In Sec. III B we shall analyze our results from this point of view. We show that the excited states populated in an EELS experiment look, on the CO moiety, like screened ion states, thus providing additional support for the approach outlined by Plummer *et al.*²⁷

In Sec. IV we apply the concepts developed for the valence excitations to recently observed core-to-bound excitations,^{30,31} and show that the same concepts can be used in the latter case. It is observed that the core-to-bound excitations are ideally suited for an analysis in terms of screening due to the localization of the core hole which is more pronounced than the localization of the valence holes. The limiting case of an equivalent core approximation leads to an appropriate description of the core-to-bound excitations. In Sec. V some remarks on the comparison of photoemission and electron-energy-loss spectroscopies are made and a final summary is given.

II. METHODS AND RESULTS

A. Experimental

The experiments were performed in a Vacuum Generator ion-pumped Auger-electron spectroscopy low-energy electron-diffraction (AES-LEED) system equipped with standard LEED optics. The base pressure was kept in the low- 10^{-10} -Torr range. The Fe(110) crystal was mounted on a temperature-controllable manipulator and cleaned by repeated sputter-anneal cycles as described elsewhere.²¹ The cleanliness of the surface before adsorption was monitored with Auger spectroscopy. Commercially available highly purified CO was used as adsorbant (2 L exposure; 1 L = 1 langmuir = 10^{-6} Torr sec). The composition of the residual gas was checked with a quadrupole mass spectrometer and the surface potentials were recorded by a vibrating capacitor. Parallel to taking the EEL spectra,

HeI photoelectron spectra using a microwave-driven uv discharge lamp³² were recorded to check whether dissociation of the adsorbate had taken place. The EEL spectra were recorded using the LEED optics as discussed in detail elsewhere by Papp.³² The primary electron energy was varied from 35 to 130 eV.

The results on the adsorbate-covered surface are shown in Fig. 2 together with the corresponding difference spectra. For comparison (see Fig. 1) the spectrum with 55 eV primary electron energy will be used exclusively for the further discussion. The series of spectra shown in Fig. 2 merely serves to demonstrate that the shoulder at 8 eV loss energy is not an artifact of one particular primary electron energy. The small intensity of the shoulder at 8 eV is probably why it is usually not observed in CO adsorbates on transition-metal surfaces. From inspection of the difference spectra it seems as if there is intensity filling in between the intense peaks at around 6 and 13 eV loss energies as the primary electron energy decreases. Whether this is due to states between 10 and 12 eV loss energy known in the free molecule cannot be decided on the basis of these experiments. Also note that the position of the maximum of the peak at ~ 13 eV loss energy seems to move to higher loss energies as the primary electron energy increases. This may be due to a redistribution of oscillator strength as a function of electron energy, indicating that several states overlap in this energy-loss region.

B. Theoretical

The basis set for the first-row atoms (C, N, and O) used in the calculations were of valence double-zeta plus polari-

zation quality.³³ For Ni, the Ar core was replaced by a modified effective potential,³⁴ the 3d, 4s, and 4p basis sets were of double-zeta quality.³⁵ The *s* combinations of *d*-type basis functions were excluded.

Calculations were carried out in the following set of molecules (states are given in parentheses): CO (ground state, $^1\Sigma^+$), CF (ground state, $^2\Pi$), NO (ground state, $^2\Pi$), CI (C $1s \rightarrow 2\pi$, $^{1,3}\Pi$), CO (O $1s \rightarrow 2\pi$, $^{1,3}\Pi$), CO ($4\sigma \rightarrow 2\pi$, $^1\Pi$), CO ($5\sigma \rightarrow 2\pi$, $^{1,3}\Pi$), NiCO (ground state, $^1\Sigma^+$), NiCO (C $1s \rightarrow 2\pi$, $^{1,3}\Pi$), NiCO (O $1s \rightarrow 2\pi$, $^{1,3}\Pi$), NiCO ($4\sigma \rightarrow 2\pi$, $^1\Pi$), NiCO ($5\sigma \rightarrow 2\pi$, $^1\Pi$), NiCO ($4\sigma + \text{Ni } 3d\pi \rightarrow 2\pi + \text{Ni } 4s$, $^1\Sigma^+$), NiCO ($5\sigma + \text{Ni } 3d\pi \rightarrow 2\pi + \text{Ni } 4s$, $^1\Sigma^+$), and NiCO (Ni $\rightarrow 2\pi$ charge transfer, $^1\Sigma^+$). The calculations on NO and CF merely serve for reference purposes when we discuss the nature of the excited states of CO and NiCO. In all calculations the GVB perfect-pairing (PP)³⁶ wave functions were first obtained. The orbitals were required to have C_{2v} symmetry. The three bonds in CO (one σ and two π bonds) were pairwise-correlated. For the ground state of the NiCO cluster, which has been shown to have $^1\Sigma^+$ symmetry,^{24,37} six pairs in total were formed, namely three pairs on the CO moiety and three pairs on the Ni (the four Ni-electrons with δ symmetry remained uncorrelated).

For all the excited states of NiCO the wave functions contained five correlated pairs plus two open-shell orbitals. Again, the three CO bonds were pairwise-correlated. For the state of Π symmetry the four Ni $3d\pi$ electrons were pairwise-correlated. The excited states of NiCO with Σ symmetry correspond to doubly excited molecules with respect to the ground state, because in addition to the $\sigma \rightarrow 2\pi$ excitation on the CO moiety a $3d\pi \rightarrow 4s$ excitation

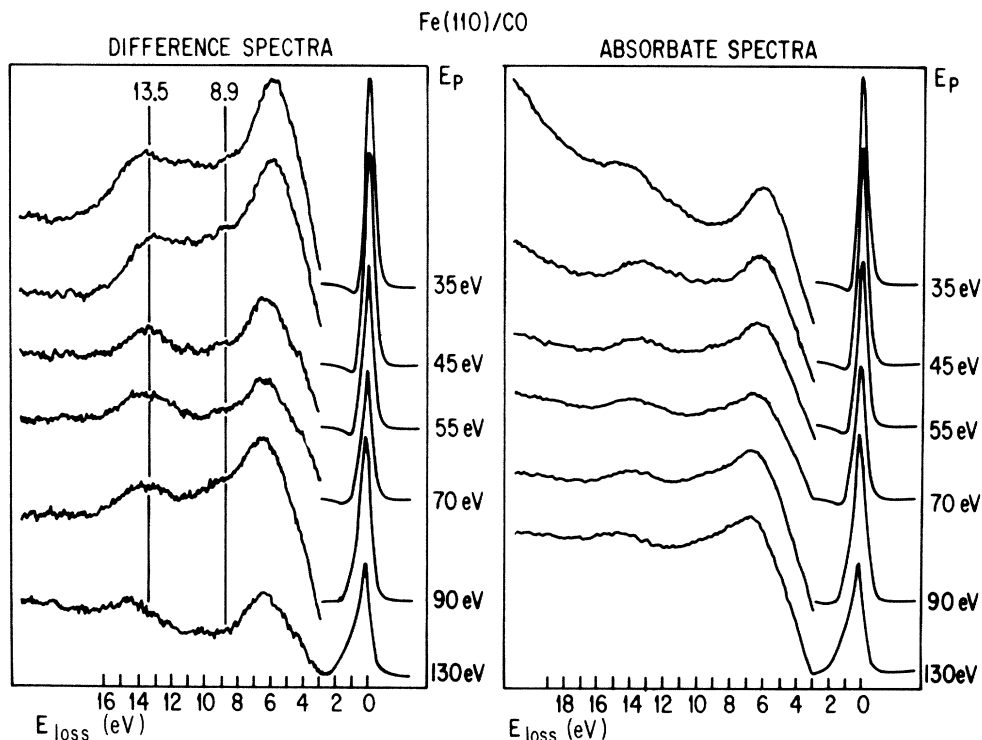


FIG. 2. Electron-energy-loss spectra and difference spectra of CO/Fe(110) for six different primary electron energies (E_p). The positions of the peaks used for discussion in the text are indicated in the difference spectra.

takes place on the Ni atom. Of the remaining three Ni $3d\pi$ electrons, two are correlated to form a pair and the third one is pairwise-correlated with the 2π electron on the CO moiety. The Ni $4s$ electron as well as the CO σ electron are treated as open shells. The only Σ state treated differently is the NiCO charge-transfer excited state. Here, in addition to the three correlated pairs on the CO moiety only two Ni $3d\pi$ electrons were pairwise-correlated. One $3d\pi$ electron was transferred to the CO 2π orbital and the other one remains on the metal atom, thus forming two open shells, which are singlet-coupled. By choosing the procedure of only correlating the $3d\pi$ electrons for all the excited states, we feel that we adequately treat Σ and Π states on the same footing at the least expense. In particular, the accuracy of the excitation energies are comparable to each other and thus should be meaningful if one is interested in investigating trends.

The wave functions generated using the GVB-PP calculations for excited states may not represent pure eigenfunctions for the states under consideration.³⁶ These wave functions are, in general, not orthogonal to lower states of the same symmetry (e.g., for the Π states), and in the case of the Σ states they may contain contamination from Δ states due to the chosen C_{2v} symmetry. Therefore the states have to be orthogonalized and symmetry-projected, respectively. This is accomplished by a limited CI calculation in a nonorthogonal basis, i.e., the resonating GVB (RGVB) (Ref. 38) procedure. The final wave functions that one calculates in this manner are approximations to pure spectroscopic states. The excitation energies calculated from RGVB are, of course, upper bounds to the true excitation energies. This means that we cannot expect the results to be as reliable as those of a full CI calculation,³⁹ but we regard the trend reflected in the results to be comparable with experimental results in a semiquantitative manner.

Figure 3 shows diagrammatically our results for the excitation energies from the ground state of free and coordinated CO to two valence excited states. These latter excited states involve the excitation of a 5σ or 4σ electron of CO into the unoccupied 2π orbital. The result for free CO is shown in the middle. On the left-hand side the results for the Σ states are shown for two different Ni—CO bond lengths, namely 1.52 Å (optimized geometry value for the ground state)²⁴ and 1.65 Å. On the right-hand side the results for the Π states are displayed. The energy is referenced to the sum of total energies of the infinitely separated CO and Ni (with the Ni in its $3d^9 4s$ configuration 3D). States involving the same electronic excitations are connected by dashed lines. The excitation energies are given in Fig. 3. The excitation energies from the ground state of NiCO to the charge-transfer state is 8.2 eV. The excitation energy from the ground state of CO to the $^3\Sigma^+(5\sigma \rightarrow 2\pi)$ state is 5.6 eV, with a calculated singlet-triplet splitting of 3.2 eV for the $5\sigma \rightarrow 2\pi$ excitation.

III. DISCUSSION

A. CO gas-phase valence spectrum

There have been several theoretical attempts to assign the gas-phase spectrum of CO. Among them are the pa-

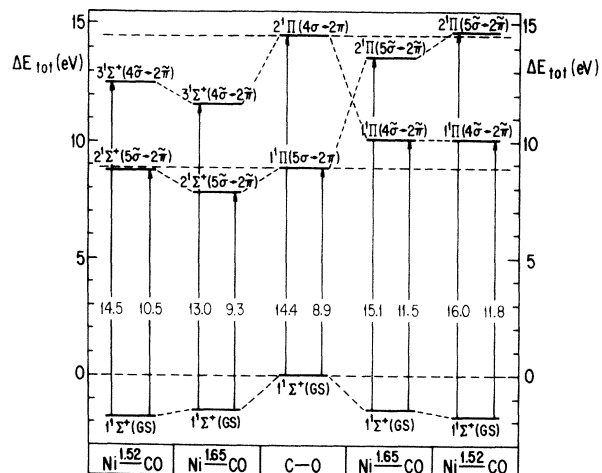


FIG. 3. Total energy level diagram for $5\sigma \rightarrow 2\pi$ and $4\sigma \rightarrow 2\pi$ excitations in CO and NiCO at two metal-CO bond lengths (1.52 and 1.65 Å) using the RGVB procedure. The zero of the energy scale refers to the sum of total energies of CO and Ni at infinite separation. The excitation energies are given as total energy differences between the two states involved in a transition (connected by an arrow). GS represents the ground state. The CO bond length was kept at 1.16 Å for all calculations.

pers by Åsbrink *et al.*¹⁷ using the semiempirical HAM3-algorithm, *ab initio* calculations by McKoy and co-workers,¹⁸ Rauk and Barriol,¹⁹ and Cooper and Langhoff.²⁰ Table I shows the assignments of the experimentally observed transitions in CO up to 14 eV (Fig. 1) excitation energy on the basis of those papers. The first peak (at ~ 6 eV loss energy) in the spectrum at the bottom of Fig. 1 (multiplied by 10^3) is due to the $5\sigma \rightarrow 2\pi$ ($a^3\Pi$) excitation with triplet spin coupling. The second transition at ~ 8.5 eV is due to the same excitation with singlet spin coupling ($A^1\Pi$). Relative to the $A^1\Pi$ state, the $a'^3\Sigma^+$ state resulting from the $1\pi \rightarrow 2\pi$ excitation is much too low in intensity to be visible. The two pairs of states of Σ^+ symmetry and Δ symmetry are hidden in the vibrational tail of the $A^1\Pi$ excitation. Their oscillator strengths are expected to be very small. At 10.8 and 11.4 eV two sharp peaks are observed which, on the basis of *ab initio* calculations^{18–20} are due to Rydberg transitions with $\sigma \rightarrow \sigma^*$ character. The $^3\Pi$ state resulting from the $4\sigma \rightarrow 2\pi$ excitation is predicted to be in this energy region but is expected to be of low intensity and not visible. Cooper and Langhoff²⁰ place the $^1\Sigma^+$ state originating from the $1\pi \rightarrow 2\pi$ valence excitation in this energy range, while Åsbrink *et al.*¹⁷ expect this excitation at 13.2 eV excitation energy. Even though the semiempirical calculation¹⁷ predicts transition energies that are too large, one may argue that the $1\pi \rightarrow 2\pi$ excitation leads to losses in the (12–13)-eV energy range.¹⁷ Above 12 eV loss energy one expects a variety of transitions corresponding to Rydberg excitations⁴⁰ and the $4\sigma \rightarrow 2\pi$ ($^1\Pi$) valence excitation. As mentioned above, the assignment of valence excitations to this loss-energy region is consistent with the findings of Hinz² that only slight changes are observed upon condensation of the gas into a molecular solid. The peaks as-

TABLE I. Observed and calculated transition energies for free CO.

(Ref. 40)			AFL	RSM	RB	CL
Symmetry	Energy	Type	(Ref. 17)	(Ref. 18)	(Ref. 19)	(Ref. 20)
$A^1\Pi$	8.07	$5\sigma \rightarrow 2\pi$	8.1	8.5	8.62	8.21
$a^3\Pi$	6.04	$5\sigma \rightarrow 2\pi$	5.9	6.0		6.06
$Z^1\Sigma^+$	~ 13.2	$1\pi \rightarrow 2\pi$	13.1			11.49
$D^1\Delta$	8.17	$1\pi \rightarrow 2\pi$	10.1	10.0	10.04	
$I^1\Sigma^-$	8.07	$1\pi \rightarrow 2\pi$	9.5	9.8	9.52	8.07
$e^3\Sigma^-$	7.96	$1\pi \rightarrow 2\pi$	9.5	9.5		
$d^3\Delta$	7.58	$1\pi \rightarrow 2\pi$	8.9	8.9		
$a'^3\Sigma^+$	6.92	$1\pi \rightarrow 2\pi$	8.4	7.9		
$(G)H^1\Pi$	13.12	$4\sigma \rightarrow 2\pi$	13.3			
$^3\Pi$	11.79	$4\sigma \rightarrow 2\pi$	11.9			
$B^1\Sigma^+$	10.78	$\sigma \rightarrow \sigma_R^*$		11.4	11.95	10.88
$C^1\Sigma^+$	11.39	$\sigma \rightarrow \sigma_R^*$		11.4	12.67	11.68
$E^1\Pi$	11.52	$\sigma \rightarrow \pi_R^*$			12.63	

signed to Rydberg states on the basis of Table I are strongly attenuated upon condensation. The losses observed in the gas phase in the region between 10 and 12 eV excitation energy degenerate to a broad shoulder while the losses due to valence excitations persist in the solid. It should be mentioned at this point that it is very unlikely, in contrast to the proposal of Lopez-Sancho and Rubio,¹¹ that any of the peaks in the gas-phase loss spectra is due to electron-induced ionization because the first adiabatic ionization potential of free CO is 14 eV (Ref. 40) and thus is in a region where the oscillator strengths of the loss features are decreasing.

B. Chemisorbed CO valence spectra

Having established an assignment for the gas-phase CO loss spectrum we are now in a position to discuss the loss spectra of chemisorbed CO. From Fig. 1 we see that, upon CO adsorption, adsorbate-induced loss peaks are found with maxima at around 5–6, 8–9, and 13–14 eV, independent of the heat of adsorption [e.g., from CO/Cu to CO/Ni, CO/Pd, or CO/Fe the heat of adsorption changes by about a factor of 2–3 (Ref. 41)]. Very clearly the peak between 13 and 14 eV remains at basically the same position as in the gas-phase and condensed-phase spectra. Note, that the lowest ionization potential of chemisorbed CO with respect to the vacuum level is close to 15 eV [Ni(111)/CO].^{42–44} Therefore the 13-eV peak cannot be due to CO ionization. In the spectrum of Spitzer and Lüth⁴ a shoulder at 11 eV loss energy is visible (as for the condensed solid case) although the spectrum was taken for a monolayer coverage. The spectrum of CO/Cu(100) shows considerably higher resolution than other spectra in this energy range. It is quite possible that remnants of the Rydberg states observed for the condensed solid are also present in this case. For the more strongly bound cases of CO on Ni, Pd, and Fe, these Rydberg states are either not resolved or are attenuated by the stronger interaction of the molecule with the surface as argued by Netzer *et al.*⁸ A particularly interesting spec-

trum is from the adsorption of CO on a Cu film studied by Avouris *et al.*³ using a high-resolution spectrometer. For rather low primary electron energies they find two peaks, one at around 6 eV and the other between 8 and 9 eV. The peak at 6 eV loss energy is considerably less intense than the one between 8 and 9 eV. It is important to note that the authors observe the peak maxima at almost identical loss energies for both monolayer and double-monolayer coverages. The only difference seems to be that in the latter case they are able to resolve vibrational structure similar to that found in the $5\sigma \rightarrow 2\pi$ ($^1,^3\Pi$) excitations of the condensed solid and the gas phase. Again, the energies of the peak maxima of the adsorbate losses are close to the gas-phase and condensed-phase values. The main difference in comparison to the gas phase is the high relative intensity of the 6-eV peak with respect to the (8–9)-eV peak. This was explained by Avouris *et al.*³ as due to nonoptical selection rules operative at the low primary electron energies used in the experiments. The same authors find two peaks, one at ~ 6 eV and one at ~ 8.5 eV, for CO/Ni(100) at room temperature. This is the only system with strong chemisorption, where in addition to the singlet-coupled $5\sigma \rightarrow 2\pi$ transition the triplet-coupled transition has been assigned.

In the spectrum of Fe(110)/CO, which represents a strongly chemisorbed system only the singlet-coupled peak can be identified. This is possibly due to interference with the intense charge-transfer peak at 6–7 eV excitation energy. It could also be due to a quenching of the triplet emission. The spectrum taken for the Fe(110)/CO system, however, exhibits both the singlet-coupled $5\sigma \rightarrow 2\pi$ excitation and the peak at 13 eV excitation energy assigned to the $4\sigma \rightarrow 2\pi$ transition.

Summarizing the analysis so far, we find that all transitions observed in the electron-loss spectrum of the free molecule can be identified in chemisorbed CO. If we adopt the assignment given above we come to the conclusion that for a wide variety of environments of the CO molecule—whether physisorbed or weakly or strongly chemisorbed—the absolute and relative excitation energies as observed in an electron-loss spectrum do not change

significantly from the excitation energies of the gas-phase molecule. This means that the "binding energies" of the CO molecule in the various ground and excited states (frozen-ground-state geometries) under consideration must be very similar. To be specific, the spectra of Fig. 1 suggest that independent of the heat of adsorption, the binding energy of the ground state of CO to a metal must be the same (to within the error of determining peak positions) as the binding energies of the excited states to the metal. Thus, this leaves the relative excitation energy as well as the absolute excitation energies in chemisorbed CO very similar to the corresponding quantities in gas-phase CO.

Up to this point we have considered only intramolecular excitations on the CO molecule. In addition to the peaks due to these excitations, we expect, as already suggested by Netzer *et al.*,^{8,14} charge-transfer excitations to occur. The latter excitations, of course, have no analog in the free molecule. We estimate the loss energies to be of the order of 6–7 eV for those transitions. This is the energy range marked by arrows in Fig. 1. There is, however, a problem of definitely assigning these transitions in the adsorbate spectra, because of the presence of intrinsic metal excitations in exactly the same energy region. One might argue that the analysis of difference spectra could resolve the difficulty but this would rest on the assumption that the intensity of these intrinsic metal excitations does not change upon adsorption, an assumption which is probably not valid.³ Therefore one can certainly not assign all the intensity in this energy range to charge-transfer excitations.

It is possible to make progress toward a solution of this dilemma by comparing the optical excitation spectra of transition-metal carbonyls with the loss spectra of chemisorbed CO. This is based on the premise that a small number of metal atoms should lead to a reduced contribution to the measured oscillator strength by metal excitations, and should therefore allow one to estimate the energy and intensity of charge-transfer excitations in coordinated CO systems.⁴⁵ Unfortunately, there are very few spectra reported which cover a reasonable energy range for simple transition-metal carbonyls. Schreiner and Brown²² reported the spectra of Ni(CO)₄ and Cr(CO)₆ and Dartigneuve *et al.*²³ the spectrum of Fe(CO)₅ up to an excitation energy of 6.5 eV. Dick *et al.*⁴⁶ presented an assignment of those spectra indicating that the absorption feature with a maximum between 6 and 7 eV, present in all carbonyl spectra,^{22,23} is due to metal to CO charge-transfer transitions. The molar extinction coefficient (ϵ) is of the order of 10^5 for these complexes.²² Less intense bands at ~ 5 eV ($\epsilon \sim 10^4$) were also assigned to charge-transfer transitions. Intra-atomic transitions on the metal were proposed as an assignment for the very weak bands between 5–6 eV excitation energy.⁴⁶ To our knowledge local ligand excitations in transition-metal carbonyls have not yet been observed with optical spectroscopy. However, we can try to compare the experimentally observed oscillator strengths of charge-transfer transitions in carbonyls with the oscillator strength of the intramolecular $5\sigma \rightarrow 2\pi$ excitation in the free molecule. The latter has been found to be 0.195 (Ref. 1), thus corresponding to a

molecular extinction coefficient of roughly 10^4 . This value is a factor of 10 smaller than that found for the charge-transfer transition and therefore consistent with the low intensity of the shoulder at 8.5 eV relative to the intense peak with maximum between 5 and 6 eV. Netzer²⁶ recently presented an EEL spectrum of condensed Ir₄(CO)₁₂ covering excitation energies up to 20 eV. This spectrum was very similar to the corresponding spectrum of CO/Ir(111),³² indicating that this probe sees mainly a local metal-CO interaction.

Summarizing our considerations about charge-transfer excitations we come to the conclusion that charge-transfer excitations have to be taken into account and that their excitation energy should be of the order of 6–7 eV. Combining this information with our assignment of the intramolecular excitations, we arrive at a consistent interpretation of the loss spectra over the full energy range from 0 to 15 eV excitation energy. Is it possible, however, to rationalize this assignment on the basis of concepts used in understanding the bonding of CO to a metal surface?

C. NiCO model of the valence spectra

The bonding of a CO molecule to a Ni atom arises through a σ -donor– π -acceptor bonding mechanism which results in a $^1\Sigma^+$ state.^{24,37} As previously pointed out,²⁴ the ground state of NiCO has a wave function which is a mixture of Ni $3d^{10}$ and Ni $3d^9 4s^1$ character, with the former being an important contribution. We consider here for the excited states only the individual components of the Ni-atom character which are most important in describing the excited states. This is an approximation dictated by computational considerations.

To visualize the synergetic bonding mechanism in NiCO, consider Figs. 4 and 5, which show orbital contour plots for the ground states of free CO and NiCO (Ni—CO bond length 1.52 Å), respectively. Figure 4 shows, from the bottom to top panel, the left-right correlated CO σ -bond pair (3σ), the oxygen lone pair orbital (4σ), one of the two degenerate CO π -bond pairs (1π), and the carbon lone pair orbital (5σ). The nature of these orbitals has been discussed in detail by Walch and Goddard.⁴⁷ Figure 5 shows some of the corresponding orbitals of NiCO. The 3σ and 4σ orbitals for NiCO are essentially identical to those of the CO molecule and therefore are not shown. The 5σ orbital becomes slightly polarized towards the metal. Panel (b) of Fig. 5 shows the Ni $3d\sigma + 4sp\sigma$ pair. We note that the Ni $4s$ orbital character is rather small because the metal-CO interaction favors the Ni d^{10} configuration as shown previously.²⁴ In this configuration the strong CO 5σ -Ni $4s$ repulsion is avoided as compared with a Ni atom in its $3d^9 4s^1$ configuration, and the CO molecule can come sufficiently close to the Ni atom to allow for back donation. Panel (a) of Fig. 5 shows the transfer of metal electrons into the unoccupied (in the free molecule) 2π orbital of CO, i.e., the Ni $3d\pi$ to CO 2π back donation. The other occupied Ni orbitals are not shown, since they do not contribute to the bonding.

With the above background, we are now prepared to consider the valence excited states of the system. We start

with a discussion of the $4\sigma \rightarrow 2\pi$ excitation; it is an "intramolecular" CO excitation. The excitation energy into the singlet state of the free molecule is calculated to be 14.4 eV (Fig. 3). Figure 6 shows orbital contour plots for this state. Besides the existence of two open-shell orbitals (4σ and 2π) which are shown in the two top panels, there are marked differences in several orbitals as compared with the ground state. The doubly-occupied σ orbitals and correlated orbital pairs all become polarized towards the oxygen atom due to the creation of the 4σ hole. The two 1π pairs are no longer identical (in C_{2v} symmetry) and are shown separately. While one component retains its character from the ground state the other one strongly polarizes towards the oxygen atom. The 2π electron is mainly localized on the carbon atom. The 4σ orbital delocalizes into the carbon region although its main amplitude is still on the oxygen atom. As expected, overall the $4\sigma \rightarrow 2\pi$ excitation leads to electron depletion in the σ region and to electron enrichment in the π region as compared with the ground state. Next, we consider how this excited state CO wave function interacts with a Ni atom.

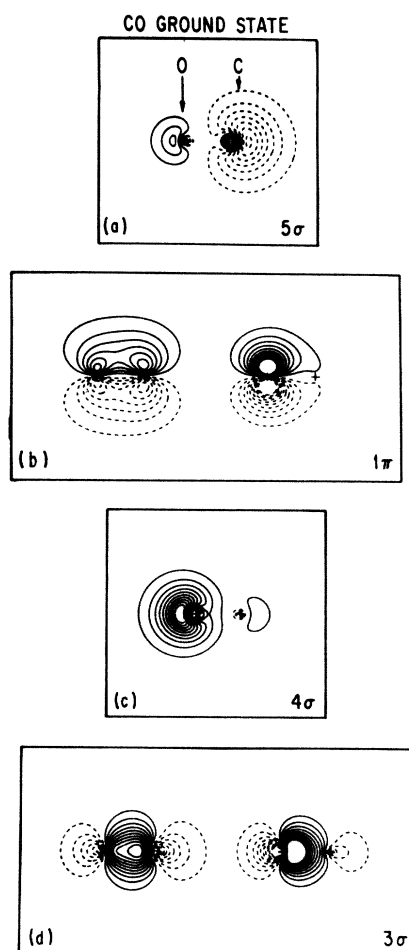


FIG. 4. One-electron orbital contour plots of the GVB-PP wave function for the ground state of the free CO molecule. Electrons which are pairwise correlated are shown within one panel. Only one of the two equivalent sets of π orbitals is shown.

In contrast to the NiCO ground state, in which the $3d^{10}$ configuration of Ni is particularly important, the NiCO excited states may have considerable $3d^9 4s^1$ character. Hence this possibility must be considered. Due to the above-mentioned electron depletion in the σ region upon excitation of the CO molecule, the repulsion between the Ni $4s$ electron and the CO carbon lone pair is reduced with respect to the ground state. Since the oxygen end of CO carries most of the π charge, the carbon end is still available for $d\pi$ back donation.

Figure 7 shows some key orbital contour plots for the $4\sigma \rightarrow 2\pi$ excited state of the NiCO cluster with the wave function restricted to only Ni $3d^9 4s^1$ character. When the resulting two open shells, i.e., Ni $4s$ and CO 4σ , which are shown in the two panels at the top [(a) and (b)], are singlet coupled, the final state has $^1\Sigma^+$ symmetry (with the proper symmetrization as described in Sec. II). Thus, the state is doubly excited with respect to the ground state of NiCO. The CO 2π orbital forms a correlated bond pair with the Ni $3d\pi$ orbital, panel (c). The CO 1π -bond pairs and the CO σ -bond pair are polarized towards the oxygen atom as in the free CO $^1\Pi$ ($4\sigma \rightarrow 2\pi$) molecule and therefore not shown in the figure. Panel (b) of Fig. 7 shows that there is still repulsion between the CO σ electrons

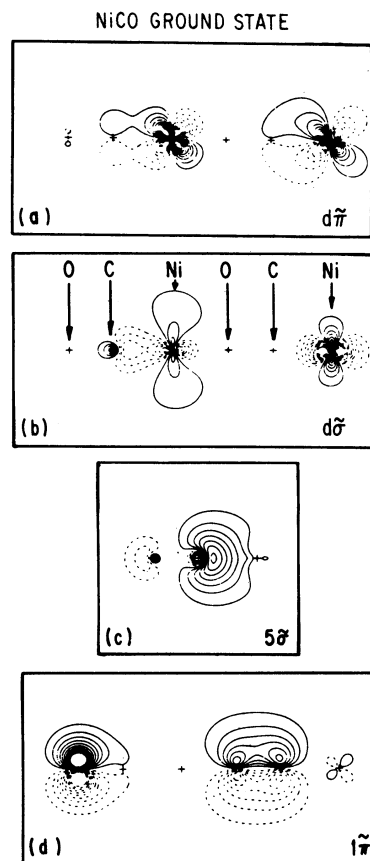


FIG. 5. One-electron orbital contour plots of the GVB-PP wave function for the ground state of NiCO at 1.52 Å metal-CO bond length. The state has Σ symmetry. Electrons which are pairwise correlated are shown within one panel. Only one of the two equivalent sets of π orbitals is shown. See the text.

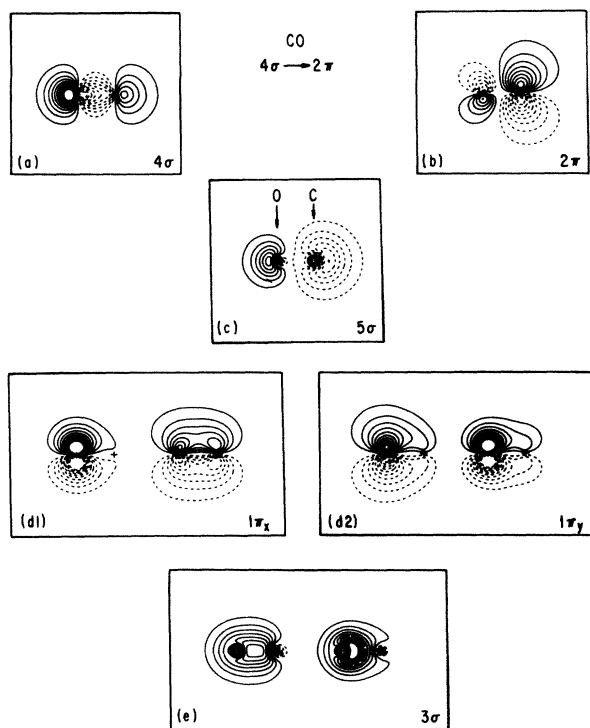


FIG. 6. One-electron orbital contour plots of the GVB-PP wave function for the $4\sigma \rightarrow 2\pi$ excited state of the free CO molecule. Electrons which are pairwise correlated are shown within one panel. The orbitals in panels (a) and (b) are open-shell orbitals which are spin coupled into a singlet.

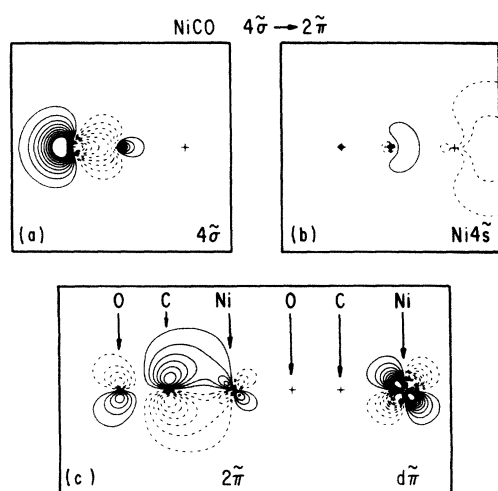


FIG. 7. One-electron orbital contour plots for some relevant orbitals of the $4\sigma \rightarrow 2\pi$ excited state of NiCO. The orbitals in panels (a) and (b) are open-shell orbitals which are spin coupled into a singlet. Panel (c) shows one of the two π bonds between the Ni atom and the CO molecule.

and the Ni 4s electron. The center of gravity of the Ni 4s electron distribution is strongly polarized away from CO so as to minimize σ repulsion. As can be seen from Fig. 3 (first column on the left-hand side), the interaction of the excited CO molecule with the Ni $3d^9 4s^1$ configuration leads to a bound state with a binding energy of 1.8 eV. This binding energy is the same as that between a ground state CO molecule and a Ni atom.²⁴ In terms of excitation energies, this means that we do not expect a drastic change when comparing the gas phase with the adsorbed CO, because the changes in binding energies in the ground and excited states for this particular excitation basically cancel out.

As already noted by Kao and Messmer,²⁴ the calculated metal-CO bond length of 1.52 Å is significantly shorter than the value experimentally suggested for CO adsorbed on Ni.⁴⁸ Thus, in order to estimate the effect of an increase in bond length on the excitation energies, we also have calculated a set of ground and excited states for NiCO using a larger metal-CO bond length of 1.65 Å. For the ground state of NiCO this leads to a weaker binding energy by 0.3 eV relative to the calculated optimized geometry. This is mainly due to a weaker back donation. For the $^1\Pi$ ($4\sigma \rightarrow 2\pi$) CO, the corresponding binding energy is ~ 2.9 eV.

A $4\sigma \rightarrow 2\pi$ excitation can also lead to a $^1\Pi$ excited state of NiCO. The orbitals for the $4\sigma \rightarrow 2\pi$ ($^1\Pi$) excited state of NiCO are not shown explicitly because the situation is very similar to the $^1\Sigma^+$ state discussed above. Except for the missing CO 5σ -Ni $4s$ repulsion and an additional CO 2π electron, the electron distributions are very similar. Due to the absence of the 5σ - $4s$ repulsion the binding energy gained is even larger compared with the earlier case. The binding energy is ~ 4.4 eV and does not change for the two metal-CO bond lengths considered (cf. Fig. 3). The excitation energy into this excited state of NiCO is between ~ 2.9 eV and ~ 2.6 eV lower than the corresponding excitation energy in the free molecule.

We turn next to a consideration of the $5\sigma \rightarrow 2\pi$ excited states. In the free CO molecule the physics is quite analogous to the one discussed for the $4\sigma \rightarrow 2\pi$ excitation. The charge polarization is now towards the carbon end of the molecule as expected for the excitation of an electron from the carbon lone pair. The polarization is not quite as strong as it was for the 4σ transition, due to the more diffuse atomic orbitals on carbon as compared to oxygen. The calculated excitation energies are 8.9 eV for the singlet transition and 5.6 eV for the triplet transition. As the polarization in the π orbitals is more towards the carbon atom, we expect the π back donation (important in NiCO for the case of the $4\sigma \rightarrow 2\pi$ excitation) to be hampered for the $5\sigma \rightarrow 2\pi$ excitation. One immediately sees the consequence of this from Fig. 3 by looking at the two columns on the right-hand side. The localized $d\pi$ electrons on the metal atom and the carbon 2π electron repel each other leading to a strong destabilization of the $5\sigma \rightarrow 2\pi$ excited $^1\Pi$ states of the NiCO cluster. The Π state is unbound by ~ 5 –6 eV (depending on the metal-CO distance), leading to an average excitation energy of 15.5 eV. If, however, we consider the $^1\Sigma^+$ state arising from the $5\sigma \rightarrow 2\pi$ excitation, the molecule is bound. By having one $d\pi$ electron

less on the Ni atom the repulsion is reduced. The Ni 4s electron is highly polarizable and shifts its center of charge so as to avoid the σ electrons of CO. This leads to a bond energy of 0.15 eV at a metal-CO distance of 1.52 Å and a bond energy of 1.05 eV at 1.65 Å. The excitation energy that we calculate for the $5\sigma \rightarrow 2\pi$ excitation into the $^1\Sigma^+$ state is ~ 9.9 eV (average of the results at the two distances) which is about 1 eV higher than calculated for the gas phase.

There is also a charge-transfer (CT) state of $^1\Sigma^+$ symmetry which should be considered. Here, a Ni $d\pi$ electron has been transferred into the empty 2π orbital of CO. The Ni is then left with an open-shell $d\pi$ orbital which is singlet coupled to the unpaired 2π electron. The resulting wave function is very similar to the interaction of an NO molecule with a Ni^+ ion. The excitation energy into this state is 8.2 eV (it has been calculated only for the 1.52-Å case) which is about 1.7 eV lower than to the $5\sigma \rightarrow 2\pi$ excited Σ state discussed above.

The nature of the states considered can be simply visualized with the aid of Fig. 8, which is a schematic representation of the wave functions described above. In the left three panels the three states of CO considered in our calculations are shown. The lowest one shows the ground state. The two diagrams for the $5\sigma \rightarrow 2\pi$ and the $4\sigma \rightarrow 2\pi$ excited states exhibit significant differences in electron distributions as discussed above. In particular, there is electron depletion in the π space of the carbon atom for the latter excitation. It is this electron depletion that allows the excited state to be bound to a Ni atom in either d^{10} (Π) or d^9s (Σ) configuration. In both cases the binding is strong, and comparable to, if not larger than, in the ground state where a reasonable bond can only be established *via* the $3d^{10}$ configuration. By contrast, the $5\sigma \rightarrow 2\pi$ excited molecule has relatively high electron density on the carbon atom leading to strong repulsion when interacting with the Ni $3d^{10}$ configuration. However, it is stabilized, although not quite so much as the $4\sigma \rightarrow 2\pi$ excited molecule, when interacting with the Ni atom in the

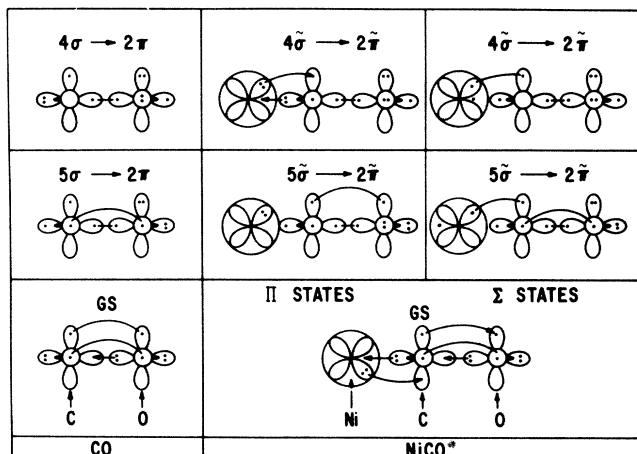


FIG. 8. Schematic representation of excited states of CO and NiCO in terms of atomic orbitals. For clarity only one $3d$ and one $4s$ orbital is shown on the Ni atom. For the two atoms of CO we show a pair of sp hybrids along the CO axis and two p orbitals perpendicular (one in the plane of the page and one perpendicular to the plane) to the CO axis. The dots represent the occupancy by electrons. Arcs connect electrons that are pairwise correlated but occupy different atomic orbitals. In the case of a polarized electron pair the polarization direction is indicated by an arrow.

$3d^9 4s^1$ configuration.

Table II compares our calculations with the assignment given above and with the experimentally observed excitation energies. The first column contains the transition energies for the most intense features in the spectrum of free CO and adsorbed CO,⁴⁹ the second column gives the assignment deduced from the collected experimental and theoretical evidence. The third column contains the numerical information presented in this work. If we compare the experimental and theoretical excitation energies for the gas phase we find that the present calculations

TABLE II. Assignment of the electron-energy-loss spectra of free and adsorbed CO and the loss energies in eV.

	Experiment (Ref. 49)	Assignment	Calculations
CO gas phase	~ 6	$^3\Pi(5\sigma \rightarrow 2\pi)$	5.6
	~ 8.5	$^1\Pi(5\sigma \rightarrow 2\pi)$	8.9
	~ 10.8	Rydberg	14.4 eV
	~ 11.5		
	~ 13.0 eV		
CO adsorbate	~ 4 – ~ 7	CT ^a	8.2 (1.52 Å) ^b
	~ 6	$^3(5\sigma \rightarrow 2\pi)$	9.9 (avg.) ^c $^1\Sigma^+$
	~ 8.0 – 9.0	$^1(5\sigma \rightarrow 2\pi)$	
	(~ 11)	Rydberg	11.7 (avg.) $^1\Pi$ 13.7 (avg.) $^1\Sigma^+$ 15.5 (avg.) $^1\Pi$
	~ 12.5 – 13.5	$^1(4\sigma \rightarrow 2\pi)$	

^aCharge-transfer transition.

^bCalculation has been done for this bond length only.

^cAverage over calculated excitation energies at 1.52 and 1.65 Å.

overestimate the excitation energies for the singlets and underestimate those for the triplets.

The calculations support the assignment of the intense feature at ~ 13 eV as mainly due to the $4\sigma \rightarrow 2\pi$ excitation of the CO molecule, but it would appear there are two final states contributing to the spectrum. The region of lower loss energy seems to be due to the $^1\Pi$ state, the region of higher loss energy to the $^1\Sigma^+$ state.⁵⁰ In order to assess the importance of these two states in the spectrum, it would be necessary to have theoretical estimates for the oscillator strengths; unfortunately, we cannot calculate these at present. There is an experimental hint, however, that there may be more than one excitation contributing to the 13-eV spectral feature, namely, the shift of the peak maximum upon changing the primary electron beam energy. A study of the angular dependence¹⁶ of the distribution of oscillator strength could help to unravel the problem since the Π and Σ final states should have different angular scattering cross sections. According to our calculations it is also possible that the $5\sigma \rightarrow 2\pi$ excitation contributes to the high energy part of the loss peak, however, this state may be autoionizing in nature. From this discussion it should be clear that the determination of intensities is an important issue which needs to be addressed in future studies in order to provide unambiguous assignments. In the gas phase the angular dependence of differential cross sections is significant,⁵¹ but for oriented molecules on a surface these dependencies are likely to be more pronounced.⁵² Thus, the experimental and theoretical study of these dependencies should be an important future concern in the interpretation of electronic EELS.

The very weak peak between ~ 8.5 – 9.5 -eV loss energy has to be assigned to the $^1\Sigma^+$ state with $5\sigma \rightarrow 2\pi$ character. The most intense feature in the whole spectrum (centered around 7-eV loss energy) is due then to charge-transfer excitations. We discussed above one specific type of charge-transfer state which may be contributing to the spectral features. Intensity borrowing into these charge-transfer states may be a reason for the small intensity of the $5\sigma \rightarrow 2\pi$ excitation itself.

It is clear that the calculated results presented in Table II do not provide a definitive assignment of the spectrum. However, it is not the objective of this study to present quantitative numerical agreement between theory and experiment, but rather to discuss possible explanations for the experimental observations based on a simple theoretical model. With these limitations in mind, we consider the results for the adsorbed molecule to be reasonable and instructive.

IV. CORE-TO-BOUND SPECTRA

Recently, core-to-bound excited states of coordinated molecules have been observed using synchrotron radiation^{30,31} tuned to the C $1s \rightarrow 2\pi$ and O $1s \rightarrow 2\pi$ excitation energies of free CO and adsorbed CO on Ni and Cu surfaces. The results show almost no change in excitation energy compared to the gas phase for the C $1s \rightarrow 2\pi$ excitation and a decrease of ~ 2 eV for the O $1s \rightarrow 2\pi$ excitation. If one takes the first moments²⁷ of the relatively broad peaks for the adsorbed molecule on Ni(111) the de-

crease in the O $1s \rightarrow 2\pi$ excitation energy persists (~ 1 eV) but there is even a slight increase in excitation energy (~ 0.5 eV) for the C $1s \rightarrow 2\pi$ excitation.

In the following we analyze these results transferring concepts derived for the valence excitations to the core-to-bound excitations. The obvious difference between valence and core-to-bound excited states is the localized nature of the core hole of the latter. In order to understand the spectroscopic properties of core-to-bound excited states of free molecules the equivalent-core approximation⁵³ has been successfully applied in the past. The equivalent core analogues for C $1s \rightarrow 2\pi$ and O $1s \rightarrow 2\pi$ excited molecules are NO and CF, respectively. Inspection of the orbital contour plots for the O $1s \rightarrow 2\pi$ excited state of CO in Fig. 9 and the ground state of CF (not presented here) show that the two sets of valence orbitals are virtually identical, indicating that we can look at the core-to-bound excited CO molecule as having the electron distribution of CF. Compared with the ground state of CO (Fig. 4) this leads to an accumulation of electronic charge on the oxygen atom. Qualitatively, this is similar to the situation found for the $4\sigma \rightarrow 2\pi$ excitation discussed above. Even though a 2π orbital which had a large amplitude on the carbon atom becomes occupied in the excita-

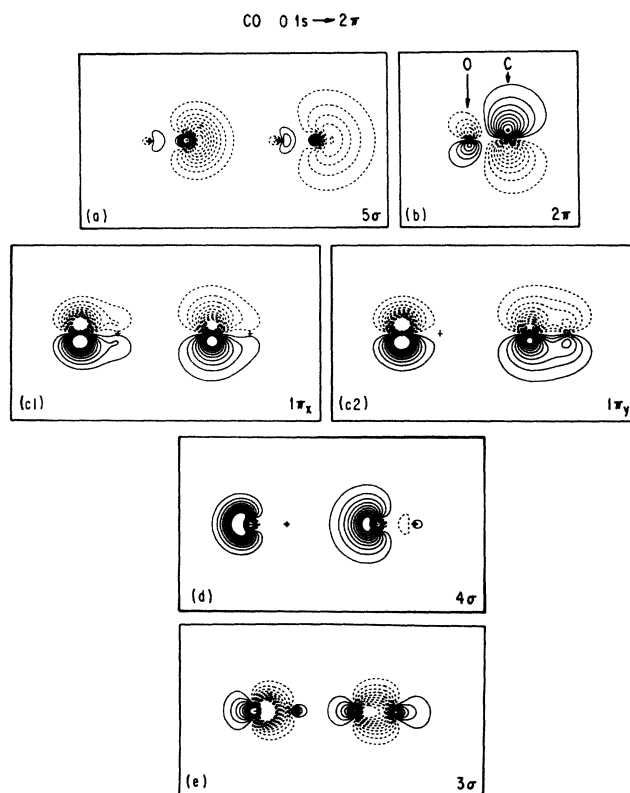


FIG. 9. Orbital contour plots of the GVB-PP wave function for the O $1s \rightarrow 2\pi$ excited state of CO. The orbital in panel (b) is an open-shell orbital. The O $1s$ open-shell orbital is not shown. Then two open-shell orbitals are spin coupled into a singlet.

tion process the 1π electrons are polarized towards the oxygen atom so that as a net effect the π -space electron population near the carbon atom is somewhat depleted with respect to the ground state. Due to the localization of the O $1s$ hole there is, of course, no depletion in the valence σ system. Using Fig. 9 it is not difficult to imagine what happens when this core-to-bound excited molecule interacts with a metal atom. The core excited molecule will be bound similarly to the $4\sigma \rightarrow 2\pi$ excited molecule. This leads to a stabilization of the excited state with respect to the ground state and results in a shift of the excitation energies to lower values as observed experimentally.

For the C $1s \rightarrow 2\pi$ excited state, on the other hand, we expect either no shift or a shift of opposite sign upon binding to a metal atom. The core-to-bound excited molecule looks like the equivalent core analog (NO), leading to an accumulation of electronic charge on the carbon atom. The ability to establish a bond towards a metal atom through back donation is therefore reduced and this reduces the bond energy of the excited state with respect to the ground state. As a consequence the excitation energy should increase.

At this point a comment is necessary concerning the coupling of the excited molecule with a metal atom in different electronic configurations. In the case of the valence excitations the σ valence-electron region is depleted in charge. This depletion favors the interaction of the excited molecule with the $4s^1 3d^9$ configuration of the metal atom. Therefore, although the metal atom is predominantly in a $3d^{10}$ configuration in the ground state of the NiCO system, valence excitation of the molecule can lead to a relaxation of the electronic configuration on the Ni atom. In the present case of core-to-bound excitations the situation is different. As stated above, the valence-electron σ depletion does not occur and therefore the electronic configuration on the Ni atom is likely to remain largely d^{10} in character. Therefore, for the core-to-bound excitations of CO adsorbed on a metal surface we consider only one set of final states ($^1\Pi$). To what degree the observed large linewidth, particularly for the O $1s \rightarrow 2\pi$ excitation in the coordinated case, is related to the electronic relaxation processes involving various configurations of the metal atom cannot be answered on the basis of the present calculations, but such effects cannot be dismissed.

Our comments on singlet-triplet splittings, made in connection with the valence excitations should hold for the core-to-bound excitations. Here, the situation is even simpler in that we only consider Π states. We have calculated singlet-triplet splittings for the gas phase as well as for the coordinated cases. For the gas phase the value for the splitting of the C $1s \rightarrow 2\pi$ states (1.37 eV) is more than 4 times as large as that for the O $1s \rightarrow 2\pi$ (0.27 eV) indicating, in agreement with calculations by Bagus and Seel,⁵⁴ and experimental results (1.4 eV versus 0.3 eV)²⁸ that the 2π orbital is more localized on the carbon atom. For the chemisorbed case we calculate 0.78 eV for the carbon excitation and 0.22 eV for the oxygen excitation, thus providing computational evidence for the qualitative conclusions derived above. A more extended discussion of these results and applications of this analysis will be published elsewhere.⁵⁵

V. SUMMARY

As alluded to in the Introduction, photoemission and electron-energy-loss spectroscopy exhibit certain common aspects.²⁷ It is the nature of the final-state wave function that allows one to connect the two spectroscopies. Due to the screening processes which occur in a photoionization event, the CO moiety looks like an excited state of the neutral molecule, with the hole transferred to the metal. The screening process is so efficient that even ionizations of CO valence electrons lead to final states with 2π occupation. While electronic excitations, at least in the optical regime, have to conserve spin, the charge-transfer screening mechanism in photoemission is not restricted by these selection rules. Thus, the screening electron assumes the lowest energy state when it couples to the molecular electrons. Although the net electronic processes in photoemission may be similar to those in EELS, the energy differences in the spectral features of the two can arise from different spin couplings in the final state of an electronic excitation compared with an electron transfer due to screening.

We have argued in the present study that the main features of electron-energy-loss spectra of valence and core excited states of adsorbed CO can be understood on the basis of a local cluster model. The results of GVB/CI calculations suggest how the observed (valence and core) excitation energies of adsorbed CO are similar to those observed for free CO. The bond energy gained by bonding the molecule in various excited states to a metal atom is very similar to the bond energy of the adsorbed molecule in its ground state. For certain molecular valence excitations the importance of including electronic relaxation processes on the metal atom has been demonstrated. For example, the $5\sigma \rightarrow 2\pi$ excited CO molecule favors the interaction with a Ni atom in the $3d^9 4s^1$ configuration while the molecule in its ground state is bound *via* interaction with a Ni atom which is largely $3d^{10}$ in character.

Qualitative arguments for the interpretation of shifts observed for core-to-bound excitations of CO upon adsorption have been presented. While an O $1s \rightarrow 2\pi$ excited molecule allows for nonrepulsive interactions *via* $d\pi$ metal back donation to the CO molecule, which leads to a stabilization of the excited state, the C $1s \rightarrow 2\pi$ excited molecule does not allow for this interaction and thus leads to a destabilization of the final state. Accordingly, one expects the excitation energies to shift to lower values upon O $1s$ excitation, and to higher values upon C $1s$ excitation which is consistent with the experimental observations of Yugnet *et al.*³⁰ For the core-to-bound excited states we have calculated the singlet-triplet splittings explicitly and found that the rather large value for the carbon excitation decreases when the molecule is coordinated to a metal atom.

Finally, we have compared the nature of the final states of electronic excitations with those observed in a photoemission experiment. Due to the similar form of the wave function on the CO moiety in both cases, one can justify the comparison between electronic excitation energies and ionization energies relative to the Fermi energy as recently proposed by Plummer *et al.*⁶ It was noted, that for the

comparison of photoemission and electron-energy-loss spectroscopy the separation of singlet and triplet states of a particular excitation is important.

ACKNOWLEDGMENTS

We are grateful to Professor E. W. Plummer for many stimulating discussions on the subject of this paper. This

work was carried out while H.J.F. was visiting the General Electric Research and Development Center. He would like to express his sincere gratitude for the financial support as well as for the hospitality accorded to him. This work was supported in part by the U. S. Office of Naval Research.

*Permanent address: Institut für Physikalische und Theoretische Chemie der Universität Erlangen-Nürnberg, Egerlandstr. 3, 8520 Erlangen, Federal Republic of Germany.

- ¹E. N. Lasette, *Can. J. Chem.* **47**, 1733 (1969).
- ²H.-J. Hinz, in *Proceedings of the IVth Conference on Vacuum Ultraviolet Radiation Physics*, edited by E. E. Koch *et al.* (Pergamon, New York, 1975).
- ³(a) Ph. Avouris, N. J. DiNardo, and J. E. Demuth, *J. Chem. Phys.* **80**, 491 (1984); (b) Ph. Avouris and J. E. Demuth, *Surf. Sci.* (to be published).
- ⁴A. Spitzer and H. Lüth, *Surf. Sci.* **102**, 29 (1981).
- ⁵B. E. Koel, D. E. Peebles, and J. M. White, *Surf. Sci.* **125**, 739 (1983); J. Küppers, *ibid.* **36**, 53 (1973).
- ⁶S. D. Bader, J. M. Bakely, M. B. Brodsky, R. J. Friddle, and R. L. Panosh, *Surf. Sci.* **74**, 405 (1978).
- ⁷W. Spiess, Ph.D. dissertation, Universität Erlangen-Nürnberg, 1984.
- ⁸F. P. Netzer, R. A. Wille, and J. A. D. Matthew, *Solid State Commun.* **21**, 97 (1977).
- ⁹K. Akimoto, Y. Sakisaka, N. Mishijima, and M. Onchi, *Surf. Sci.* **88**, 109 (1979).
- ¹⁰Y. Sakisaka and M. Onchi, *Surf. Sci.* **108**, L403 (1981).
- ¹¹J. M. Lopez-Sancho and J. Rubio, *Surf. Sci.* **108**, L403 (1981).
- ¹²M. A. Chesters, B. J. Hopkins, and R. I. Winton, *Surf. Sci.* **59**, 46 (1976).
- ¹³G. M. Rubloff and J. I. Freeouf, *Phys. Rev. B* **17**, 4680 (1978).
- ¹⁴F. P. Netzer and J. A. D. Matthew, *Surf. Sci.* **81**, L651 (1979).
- ¹⁵S. Ishi and Y. Ohno, *Surf. Sci.* **139**, L219 (1984).
- ¹⁶F. P. Netzer, J. U. Mack, E. Bertel, and J. A. D. Matthew, *Surf. Sci.* **160**, L509 (1985).
- ¹⁷L. Åsbrink, C. Fridh, and E. Lindholm, *Chem. Phys.* **27**, 159 (1978).
- ¹⁸C. W. McCurdy, Jr., T. N. Resigno, D. L. Yeager, and V. McKoy, in *Methods of Electronic Structure Theory*, edited by H. F. Schaefer III (Plenum, New York, 1977); J. Rose, T. Shibuya, and V. McKoy, *J. Chem. Phys.* **58**, 74 (1973).
- ¹⁹A. Rauk and J. M. Barriol, *Chem. Phys.* **25**, 409 (1977).
- ²⁰D. M. Cooper and S. R. Langhoff, *J. Chem. Phys.* **74**, 1200 (1981).
- ²¹G. Wedler, W. Spiess, and H. Behner (unpublished).
- ²²A. F. Schreiner and T. C. Brown, *J. Am. Chem. Soc.* **90**, 3366 (1968).
- ²³M. Dartigneuave, Y. Dartigneuave, and H. B. Gray, *Bull. Soc. Chim. Fr.* 4223 (1969).
- ²⁴C. M. Kao and R. P. Messmer, *Phys. Rev. B* **31**, 4835 (1985).
- ²⁵H.-J. Freund, R. P. Messmer, C. M. Kao, and E. W. Plummer, *Phys. Rev. B* **31**, 4848 (1985).
- ²⁶F. P. Netzer, Trieste Symposium on Adsorbate Spectroscopies, Trieste, 1984 (unpublished).
- ²⁷E. W. Plummer, C. T. Chen, W. Ford, W. Eberhardt, R. P. Messmer, and H.-J. Freund, *Surf. Sci.* **158**, 58 (1985).
- ²⁸L. Ungier and T. D. Thomas, *Chem. Phys. Lett.* **96**, 247 (1983).
- ²⁹A. P. Hitchcock and C. E. Brion, *J. Electron Spectrosc.* **18**, 1 (1980).
- ³⁰J. Yugnet, F. J. Himpsel, Ph. Avouris, and E. E. Koch, *Phys. Rev. Lett.* **53**, 198 (1984).
- ³¹E. W. Plummer, C. T. Chen, and W. Ford (unpublished).
- ³²H. Papp, *Ber. Bunsenges. Phys. Chem.* **86**, 555 (1982).
- ³³T. H. Dunning, Jr. and P. J. Hay, in *Methods of Electronic Structure Theory*, edited by H. F. Schaefer III (Plenum, New York, 1977), Vol. 3, pp. 1–27.
- ³⁴T. H. Upton and W. A. Goddard III, in *Chemistry and Physics of Solid Surfaces*, edited by T. Vanselow and W. England (CRC Press, Boca Raton, 1982), Vol. 3, pp. 127–162.
- ³⁵The double- ζ basis set for the 3d orbital was constructed from five primitives optimized for the d^{10} configuration [taken from A. K. Rappe, T. A. Smedley, and W. A. Goddard III, *J. Phys. Chem.* **85**, 2607 (1982)].
- ³⁶R. A. Bair, W. A. Goddard III, A. F. Voter, A. K. Rappe, L. G. Yaffe, F. W. Bobrowicz, W. R. Wadt, P. J. Hay, and W. J. Hunt, Program GVB2P5 (unpublished); see R. A. Bair, Ph.D. thesis, California Institute of Technology, 1980; F. W. Bobrowicz and W. A. Goddard III, in *Methods of Electronic Structure Theory*, edited by H. F. Schaefer III (Plenum, New York, 1977), Vol. 3, pp. 79–127; W. J. Hunt, P. J. Hay, and W. A. Goddard III, *J. Chem. Phys.* **57**, 738 (1972).
- ³⁷A. B. Rives and R. F. Fenske, *J. Chem. Phys.* **75**, 1293 (1981).
- ³⁸A. F. Voter and W. A. Goddard III, *Chem. Phys.* **57**, 253 (1981).
- ³⁹For a recent CI calculation on excited states of CO see, for example, Cooper *et al.* in Ref. 20.
- ⁴⁰K. P. Huber and G. Herzberg, *Molecular Spectra and Molecular Structure. IV. Constants of Diatomic Molecules* (Van Nostrand, New York, 1979).
- ⁴¹G. Ertl, in *The Nature of the Surface Chemical Bond*, edited by T. N. Rhodin and G. Ertl (North-Holland, Amsterdam, 1979).
- ⁴²K. Wandelt, *J. Vac. Sci. Technol. A* **2**, 802 (1984).
- ⁴³K. Christmann, O. Schober, and G. Ertl, *J. Chem. Phys.* **60**, 4719 (1974).
- ⁴⁴E. W. Plummer and W. Eberhardt, *Adv. Chem. Phys.* **49**, 537 (1982).
- ⁴⁵G. J. Schulz, *Rev. Mod. Phys.* **45**, 423 (1973).
- ⁴⁶B. Dick, H.-J. Freund, and G. Hohlneicher, *Mol. Phys.* **45**, 427 (1982).
- ⁴⁷S. P. Walch and W. A. Goddard III, *J. Am. Chem. Soc.* **98**, 7908 (1976).
- ⁴⁸S. Anderson and J. B. Pendry, *Surf. Sci.* **71**, 75 (1978); *Phys. Rev. Lett.* **43**, 363 (1979).
- ⁴⁹The energies given are averages over the peak positions shown in Fig. 1.

⁵⁰An assignment of the spectrum in terms of excited states labeled within $C_{\infty v}$ symmetry strictly only applies for the linear NiCO molecule.

⁵¹D. C. Cartwright, A. Chutjian, S. Trajmar, and W. Williams, Phys. Rev. A **16**, 1013 (1977).

⁵²L. M. Brescansin, M. A. P. Lima, W. M. Huo, and V. McKoy,

Phys. Rev. B **32**, 7122 (1985).

⁵³W. L. Jolly and D. N. Hendrickson, J. Am. Chem. Soc. **92**, 1863 (1970).

⁵⁴P. S. Bagus and M. Seel, Phys. Rev. B **23**, 2065 (1981).

⁵⁵H.-J. Freund, R. P. Messmer, and C. M. Kao (unpublished).